

# Molecular Design, Synthesis, and Characterization of Liquid Crystal–Coil Diblock Copolymers with Azobenzene Side Groups

Guoping Mao, Jianguo Wang, Scott R. Clingman, and Christopher K. Ober\*

Department of Materials Science and Engineering, Cornell University, Ithaca, New York 14853

John T. Chen and Edwin L. Thomas\*

Department of Materials Science and Engineering, Massachusetts Institute of Technology, Cambridge, Massachusetts 02139

Received December 4, 1996; Revised Manuscript Received March 5, 1997<sup>®</sup>

**ABSTRACT:** The synthesis and characterization of a family of well-defined liquid crystal–coil (LC–coil) diblock copolymers have been carried out. The block copolymers in this study have been designed to have nearly identical molecular weight azobenzene-containing LC blocks in order to eliminate possible variations in LC behavior caused by the differences in the LC block molecular weight. Quantitative hydroboration chemistry was used to convert the pendent double bonds of an isoprene block to hydroxyl groups to which the mesogenic groups were attached via acid chloride coupling. The LC homopolymer and the block copolymers (LC volume fraction from  $f_{LC} = 0.82$  to  $f_{LC} = 0.20$ ) all exhibited smectic mesophases with similar clearing transition temperatures. The clearing transition enthalpies strongly depend on the block composition ratio and decrease as the LC block volume fraction decreases. Solvent-casting of a lamellar LC–coil copolymer (SICN5-66/60) resulted in an oriented bulk film in which both the axes of the mesogenic groups and the lamellar interfaces lie parallel to the film surfaces. A LC cylinder morphology was observed with a  $f_{LC} = 0.22$  LC-containing block (SICN5-176/55) using TEM and confirmed by SAXS measurements. This is the first observation with the LC block in a cylinder microdomain. Other morphologies (bicontinuous, LC sphere) were observed by TEM while retaining the smectic order in the LC microphase.

## Introduction

Conventional AB coil–coil diblock copolymers such as poly(styrene-*b*-diene) have morphologies which may include spheres, cylinders, double diamond (DD), double gyroid (DG), and lamellae depending on the relative volume fractions of the two blocks.<sup>1</sup> The important parameters which govern phase separation are the total degree of polymerization ( $N = N_A + N_B$ ), the Flory–Huggins  $\chi$  parameter, and the volume fraction  $f_A$ .<sup>2</sup> Only recently has theory begun to consider the effect of chain stiffness and the effect of liquid crystalline order in block systems. If chain rigidity is increased for one block (an extreme case is the rod–coil diblock copolymer<sup>3</sup> where one block is a rigid rod), interesting zigzag and arrowhead morphologies corresponding to smectic C and smectic O structures may be observed as in the case of the rod–coil diblock copolymer poly(*n*-hexyl isocyanate-*b*-styrene).<sup>3a,3b</sup> These strikingly new morphologies developed as the rigid block of the rod–coil block copolymer organized into nematic and then smectic mesophases. These morphologies arise as a result of the interplay between phase separation and liquid crystallinity. This suggests the possibility that novel morphologies (which may lead to heretofore unencountered properties) may also be observed in new block copolymers containing a side group liquid crystal block in place of a rigid-rod block.

Liquid crystal polymers (LCPs) have undergone tremendous development over the last 20 years.<sup>4</sup> LC–coil diblock copolymers are a unique subclass of these materials and combine mesomorphic order (molecular scale) with microphase separation (supermolecular scale)

in a single polymer system. Unanswered questions include what type of microphase separated structures will form and what influences the coil block will have on LC behavior. By embedding the LC phase in a polymer matrix with different domain sizes and geometries, the mesophase must adapt to various domain boundary conditions.

Block and graft copolymers containing a LC block have been recently reviewed in detail by Chiellini et al.<sup>5</sup> Of the several types of such polymers that now exist, Gronski and co-workers<sup>6</sup> developed the first example of a symmetric LC–coil diblock copolymer by attachment of pendent cholesteryl mesogenic groups to a hydroxylated poly(styrene-*b*-1,2-butadiene) block copolymer. The clearing enthalpy of their lamellar LC–coil block copolymer was significantly lower than that of its LC homopolymer analog with a 60% loss of clearing transition enthalpy, indicating that there is indeed an influence of phase separation on liquid crystallinity. This observation was originally believed to be due to a rather disordered interfacial region between the two components.

In addition to the polymer-analogous method of synthesizing side group LC–coil block copolymers,<sup>6–8</sup> living polymerization of mesogenic monomers by various mechanisms has been widely used. Generally these living methods give modest molecular weights due to the difficulties of monomer purification. Hefft and Springer<sup>9</sup> reported an LC–coil diblock copolymer prepared by living group transfer polymerization (GTP), while Percec and Lee<sup>10</sup> used living cationic polymerization ( $DP_n = 7\sim 9$ ). Komiya and Schrock<sup>11</sup> reported a series of block copolymers with only a nematic mesophase synthesized by living ring-opening metathesis

<sup>®</sup> Abstract published in *Advance ACS Abstracts*, April 15, 1997.

polymerization (ROMP). Finkelmann et al.<sup>12</sup> and Watanabe et al.<sup>13</sup> instead employed direct anionic polymerization for the synthesis of LC–coil diblock copolymers from mesogenic methacrylate monomers. These researchers<sup>13</sup> were only able to produce LC blocks of  $\sim 15\,000$  g/mol ( $DP_n = 30\sim 40$ ) due to difficulties of monomer purification. Macroinitiator methods have also been used by Chiellini and co-workers<sup>5,14</sup> to create several architectures of LC block copolymers. However, only lamellar<sup>6,13</sup> and coil spherical morphologies<sup>12</sup> in LC matrices were reported in detail for these polymer systems.

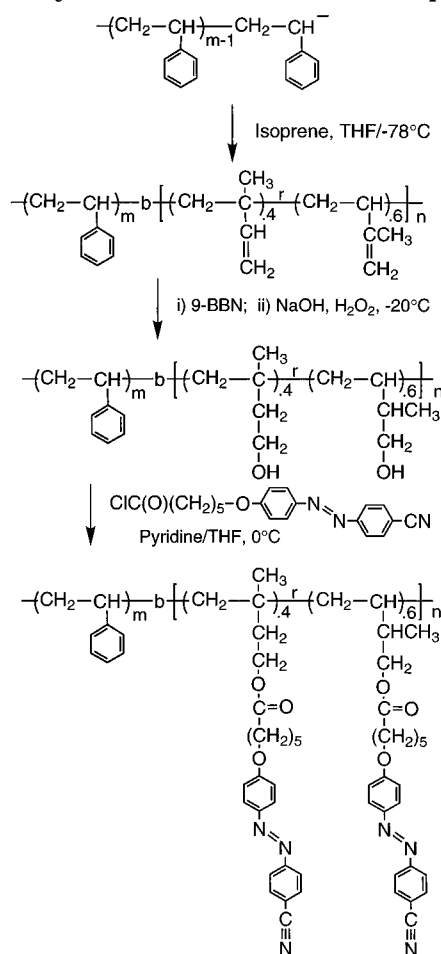
Fischer et al.<sup>7</sup> carried out a systematic study of the morphologies of LC–coil diblock copolymers using small-angle X-ray scattering (SAXS) and transmission electron microscopy (TEM). These polymers exhibited coil–sphere, coil–cylinder, and lamellar morphologies; however, a LC–cylinder morphology was not observed when the LC block was the minor component. LC spheres were observed (with LC block volume fractions less than 0.30), but only nematic mesophases were detected even though the higher molecular weight LC homopolymer exhibited a smectic mesophase. This phenomenon was explained<sup>7</sup> by pointing out that a layered smectic mesophase is not favored within a spherical microdomain morphology. However, we note that the LC blocks used in Fischer's work are quite short ( $DP_n = 6\sim 10$ ) for the polymers studied with low volume fraction LC blocks. The degree of polymerization ( $DP_n$ ) has a great influence on LC behavior, including transition enthalpy, transition temperature, and mesophase type,<sup>15</sup> independent of the microdomain structure.

The observation that there is a suppression of LC clearing transition enthalpy and the reported absence of certain morphologies suggest that the interplay between the amorphous and LC phases provides an interesting new tool for tailoring microstructure and properties. These interactions depend on the geometric constraints of mesogens at interfaces, the interface area per chain, and the thermodynamics of the mesophase balanced against phase separation. In order to address some of these intriguing issues, the LC–coil block copolymers used in our study were designed to have the same LC block length in order to eliminate that influence on the polymer properties. Polymer-analogous chemistry was used to retain precise control of the  $DP_n$  of each block so that the mesophase type could be easily tailored.<sup>16</sup> A styrene–isoprene diblock copolymer was employed as the base material and was prepared by anionic polymerization.<sup>17</sup> Polymer modification enabled the creation of different LC block structures from the same parent polymer<sup>18,19</sup> by attachment of specifically tailored carboxylic acid functionalized azobenzene mesogenic groups (Scheme 1). The synthesis and characterization of these block copolymers and a study of the relationship between their microstructure and mesophase behavior are the subject of this paper.

## Experimental Section

**I. Solvents and Starting Materials.** Unless noted, all chemicals were purchased from Aldrich and used without further purification. Tetrahydrofuran (THF) and toluene were freshly distilled from sodium/benzophenone (deep purple color) under nitrogen after refluxing for at least 7 h. Pyridine and hexane were distilled from  $\text{CaH}_2$  after refluxing for 4 h. Styrene was purified first by washing with 10% NaOH solution to remove inhibitor before stirring with  $\text{CaH}_2$  for 48 h followed by stirring with  $\text{MgBu}_2$  for 24 h until a bright greenish color appeared. The dried monomer was finally vacuum-distilled

## Scheme 1. Synthesis of LC–Coil Diblock Copolymers



into a cold trap where it could be transferred into a monomer reservoir with known volume and could be stored at  $-20\text{ }^{\circ}\text{C}$  for 1 week. Isoprene was stirred with  $\text{CaH}_2$  for 2 days at room temperature and distilled from  $\text{CaH}_2$  before stirring with  $\text{MgBu}_2$  at  $0\text{ }^{\circ}\text{C}$  for 4 h and distilled into a cold trap. It was then transferred to a monomer reservoir and used immediately.

GPC measurements were performed using a Waters GPC equipped with Ultrastaygel columns of 500-, 1000-, and 10000-Å pore sizes, and a linear column with mixed pore sizes and dual detectors [RI and UV ( $\lambda = 254$  and  $368\text{ nm}$ )] using THF as elution solvent at  $35\text{ }^{\circ}\text{C}$  with an elution rate of  $0.30\text{ mL/min}$ . Narrow dispersity polystyrenes were used as calibration standards. FT-IR was carried out on a Mattson 2020 Galaxy series instrument.  $^1\text{H}$  and  $^{13}\text{C}$  NMR spectra were made on 200 or 400 MHz Varian NMR instruments using  $\text{CDCl}_3$  as solvent. A relaxation time ( $T_1$ ) of 12 s was used for all polymer  $^1\text{H}$  NMR characterization. Thermograms were measured using a Perkin-Elmer DSC 7. Polarized optical microscopy (POM) observation was performed on a Nikon optical microscope. Thin layer chromatography (TLC) was carried out using Krackeler silica gel glass plates with fluorescent indicator. Silica gel (230–400 mesh) from Krackeler Scientific was used in flash column chromatography.<sup>20</sup> The density of the LC homopolymer was measured with a series of NaI–water solution (density 1.0–1.4) and ethylene glycol ( $1.113\text{ g/cm}^3$ ) to be  $1.15\text{ g/cm}^3$  at room temperature.

The bulk morphology of the LC–coil diblock copolymers was examined using TEM and SAXS. Films ( $\sim 1\text{ mm}$  thick) were cast from 5 wt % solutions in toluene and allowed to evaporate slowly for 1 week. The as-cast films were placed in a vacuum oven for 2 days to remove residual solvent. The samples were then annealed at  $145\text{ }^{\circ}\text{C}$  for 4 days in a vacuum oven. Thin sections ( $\sim 500\text{--}700\text{ Å}$ ) suitable for TEM were microtomed at room temperature using a Reichert–Jung FC4E Ultracut E microtome equipped with a diamond knife. To enhance the

electron density contrast between the LC and PS blocks, the sections were stained for 15 min in RuO<sub>4</sub> vapors, which preferentially stains the PS block. Bright field TEM was performed using a JEOL 200CX electron microscope operated at 200 kV.

WAXD patterns were obtained with a Statton Camera with a Ni-filtered Cu K $\alpha$  X-ray source ( $\lambda = 1.54$  Å). Samples for WAXD studies were prepared via the following methods: bulk (no orientation), solvent-casting followed by annealing, fiber-pulling from the polymer melts, and spatula-shearing or rolling in the LC states. SAXS and some of the WAXD patterns were obtained using the Cornell High Energy Synchrotron Source (CHESS) with  $\lambda = 0.899$  Å.

**II. Anionic Polymerization.<sup>21</sup> 1. Homopolymerization.** *sec*-BuLi was used as initiator in tetrahydrofuran solvent under high-purity argon. The reaction temperature was  $-78$  °C using 2-propanol/dry ice as a cooling source. A typical example is given below:

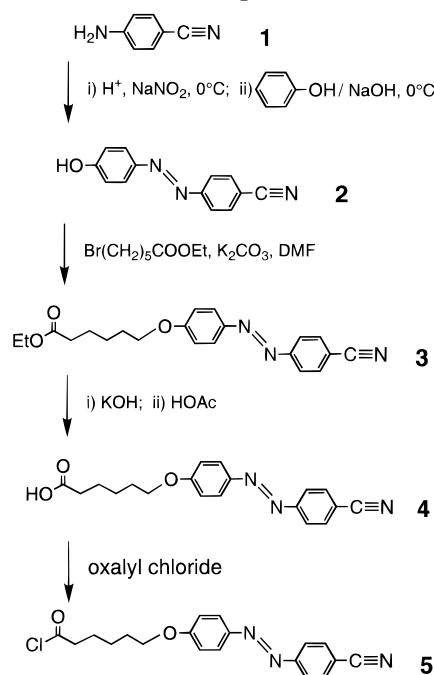
For the synthesis of **I-13** (designated as polyisoprene with a  $M_n$  of 13 kg/mol), all the apparatus was rigorously dried under vacuum with heating. THF (300 mL) was distilled into a 500 mL flask equipped with a 13 mm diameter rototflo stopcock. The solution was then cooled to  $-78$  °C using a 2-propanol/dry ice cooling bath. Thirty minutes later, 0.60 mL of *sec*-BuLi (1.3 M solution in hexane, 0.70 mmol) was added. After five additional minutes, 15 mL of isoprene (10.2 g) was transferred from the monomer reservoir to the polymerization flask via cannula. A slightly greenish yellow color soon developed. The polymerization was run for 68 h at  $-78$  °C. To kill the living polymer, 1 mL of anhydrous degassed methanol was transferred into the reaction flask. The polymer was then precipitated into methanol, filtered, washed with copious amounts of methanol, and finally dried under vacuum at room temperature for 48 h. Polymer (9.12 g) was collected. The conversion of isoprene was 89.4%. The theoretical  $M_n$  was 13 000, while GPC gives a  $M_n$  of 17 600 relative to polystyrene standards and a polydispersity ( $M_w/M_n$ ) of 1.08. Low-angle laser light-scattering (LALLS) gave a  $M_n$  of 13 500 g/mol, which is in good agreement with the theoretical value.

**2. Block Copolymerizations.** A typical example of poly(styrene-*b*-1,2- & -3,4-isoprene) block copolymerization is given below:

For the synthesis of **SI-14/13** [designated as poly(styrene-*b*-1,2- & -3,4-isoprene) block copolymer with a polystyrene (**S**)  $M_n$  of 14 kg/mol and a polyisoprene (**I**)  $M_n$  of 13 kg/mol], 120 mL of THF was distilled into a 250 mL flask equipped with a 13 mm diameter rototflo stopcock. The solution was cooled to  $-78$  °C using a 2-propanol/dry ice cooling bath. Thirty minutes later, 0.31 mL of *sec*-BuLi (1.3 M solution in hexane, 0.40 mmol) was added. After five additional minutes, 6.30 mL of styrene (5.67 g) was transferred from the monomer reservoir to the polymerization flask via cannula with vigorous stirring. A bright orange yellow color soon developed. Thirty minutes later, 1 mL of polymer solution was sampled from the polymerization solution via another cannula. Immediately after sampling, 10 mL (6.8 g) of isoprene was transferred into the polymerization flask via a new cannula. The bright orange color disappeared right away, and a very light greenish color appeared. The polymerization was then run for 74 h at  $-78$  °C. To terminate the living polymer, 1 mL of anhydrous degassed methanol was transferred into the reaction flask. The polymer was then precipitated into methanol, filtered, washed with copious amounts of methanol, and finally dried under vacuum at room temperature for 48 h. Polymer (10.72 g) was collected. The conversion of isoprene is 73.8%. For the polystyrene precursor, GPC gives a  $M_n$  of 14 400 and a polydispersity ( $M_w/M_n$ ) of 1.06; for the final block copolymer, GPC gives a  $M_n$  of 36 000 and a polydispersity ( $M_w/M_n$ ) of 1.07.

**III. Hydroborations.<sup>8,22–24</sup> Example 1: Homopolymer Poly(1,2- & -3,4-isoprene).** To make **I-13-OH** (designated as hydroxylated-polyisoprene homopolymer from 13 kg/mol polyisoprene), 2.0 g (29.4 mmol vinyl and methylvinyl groups) of homopolymer **I-13** was vacuum-dried overnight at 50 °C in a 250 mL flask equipped with a rototflo stopcock and a septum. After cooling, freshly distilled THF (40 mL) was transferred into the flask via a cannula. The solution was cooled to  $-15$

## Scheme 2. Synthesis of Mesogen with Functional Groups



°C, and 70.6 mL of 9-BBN (9-borabicyclo[3.3.1]nonane, purchased from Aldrich, 0.50 M THF solution) (35.3 mmol) was transferred in. The solution was stirred for 24 h at room temperature and then cooled to  $-25$  °C before 1 mL of anhydrous methanol was injected into the solution. After the solution was stirred for 30 min, 6.50 mL of 6 N NaOH (purged with N<sub>2</sub> for 30 min) (39.0 mmol) was added. After an additional 10 min, 13.0 mL of 30% H<sub>2</sub>O<sub>2</sub> (purged with N<sub>2</sub> for 30 min) was added, turning the solution opaque. Precipitation occurred, and stirring became difficult. After an additional 2 h at  $-25$  °C, the temperature of the solution was slowly raised to room temperature. The solution was stirred for 30 min before being heated to 55 °C for 1 h to form a "homogeneous" solution. After cooling to room temperature, the solution clearly phase-separated with an aqueous layer on the bottom. The solution was cooled with a liquid N<sub>2</sub>/2-propanol bath to freeze the aqueous phase. The clear organic layer was slowly poured into 800 mL of 0.25 M NaOH (or KOH) solution while the aqueous phase (syrup-like) containing NaB(OH)<sub>4</sub> remained in the reaction flask. The polymer (very fine precipitates) was then filtered, washed with 0.25 M NaOH solution, and dissolved in 60 mL of MeOH. The polymer solution was then reprecipitated into a 0.25 M NaOH solution and stirred overnight. The polymer was then filtered and washed with a NaOH solution and redissolved and reprecipitated 3 more times. Finally, the polymer was washed with copious amounts of water before drying under vacuum. Yield: >95% (due to filtration loss). The hydroxylated polymer was capped with acetyl chloride to enhance solubility before GPC analysis and NMR characterization. GPC showed a polydispersity of 1.09 and an  $M_n$  of 28 000 g/mol.

**Example 2: Block Copolymer.** The method for the hydroboration of block copolymer is very similar to that of the homopolymer except THF/MeOH (for a PS/PI wt ratio less than 3) or THF (for a PS/PI wt ratio higher than 3) is used instead of MeOH for dissolving the hydroxylated block copolymer. For block copolymers with a PS/PI wt ratio higher than 3, the hydroxylated block copolymer can dissolve in THF and GPC can be performed without capping of hydroxyl groups with acetyl chloride.

**IV. Synthesis of LC-Coil Diblock Copolymers Utilizing Acid Chloride (Scheme 2).** **1. 4-Cyano-4'-hydroxyazobenzene (2).** This was synthesized using the method

reported in the literature.<sup>25a,b</sup> Mp: 201 °C (lit. 203 °C).<sup>25</sup> <sup>1</sup>H NMR (DMSO-*d*<sub>6</sub>):  $\delta$  10.51 (1H, s, OH); 7.98 (4H, quartet, aromatic next to CN); 7.20 (2H, d, aromatic); 6.85 (2H, d, aromatic next to OH).

**2. Synthesis of CN5-ester (3).** 4-Cyano-4'-hydroxyazobenzene (12.8 g; 57.3 mmol), 8.7 g of K<sub>2</sub>CO<sub>3</sub> (63.0 mmol), 30 mg of KI, and 500 mL of anhydrous DMF were placed in a 1000 mL flask under N<sub>2</sub>. After the solution was heated to 90 °C for 30 min, 13.8 g of ethyl  $\omega$ -bromohexanoate (61.8 mmol) was added to the flask dropwise. The solution was then stirred at 120 °C for 3 h. After 4-cyano-4'-hydroxyazobenzene was no longer detectable by TLC, the solution was cooled and poured into 900 mL of distilled water containing 10 g of K<sub>2</sub>CO<sub>3</sub>. The precipitates were filtered and washed with water before recrystallization from 1 L of 95% ethanol. CN5-ester (19.9 g) was obtained. Yield: 95%. Mp: 131 °C. <sup>1</sup>H NMR (CDCl<sub>3</sub>):  $\delta$  7.95 (4H, m, aromatic next to CN); 7.80 (2H, d, aromatic); 7.01 (2H, d, aromatic next to ether linkage); 4.10 (4H, m, CH<sub>2</sub> next to oxygen); 1.85 (2H, t, CH<sub>2</sub> next to carbonyl group); 1.72 (2H, m, CH<sub>2</sub>); 1.55 (2H, m, CH<sub>2</sub>); 1.55 (2H, m, CH<sub>2</sub>); 1.30 (3H, t, CH<sub>3</sub>). IR (KBr pellet): 2228 cm<sup>-1</sup> (CN); 1734 cm<sup>-1</sup> (ester).

**3. Synthesis of CN5-Acid (4).** CN5-ester (3) (10 g; 27.4 mmol) was dissolved in 300 mL of anhydrous ethanol in a 500 mL flask. KOH (1.18 g; 26.03 mmol) was added, and the solution was refluxed for 3 h. After cooling, the solution was poured into 400 mL of distilled water. After filtration (to remove unreacted ester), the solution was neutralized with acetic acid to a pH of 4–5. The orange colored precipitate was then filtered and washed with copious amounts of distilled water. The product was then crystallized from ethanol. CN5-acid (4) (8.1 g) was obtained. Yield: 88%. Mp: 192.5 °C; monotropic nematic, I 191.2 °C N 167.3 °C K. <sup>1</sup>H NMR (DMSO-*d*<sub>6</sub>):  $\delta$  11.95 (1H, s, acid); 8.00 (6H, m, aromatic next to CN); 7.16 (2H, d, aromatic next to ether linkage); 4.09 (2H, t, CH<sub>2</sub> next to ether linkage); 2.20 (2H, t, CH<sub>2</sub> next to carbonyl group); 1.76 (2H, m, CH<sub>2</sub>); 1.50 (4H, m, CH<sub>2</sub>). IR (KBr pellet): 2241 cm<sup>-1</sup> (CN); 1739 cm<sup>-1</sup> (dimeric acid); 1707 cm<sup>-1</sup> (monomeric acid). It is worth noting that Aoki et al.<sup>25c</sup> utilized CN5-acid as one of the surface modifiers for their "command surface" concept. However, the detailed synthesis, mp, and LC behavior were not reported.

**4. Synthesis of CN5-acid Chloride<sup>26</sup> (5).** CN5-acid (4) (2.0 g) was vacuum-dried at 1 mTorr for 2 h. Anhydrous toluene (15 mL) and 4 mL of oxalyl chloride were then added to the flask. The suspended solution was stirred at room temperature for 30 min before refluxing for 3 h until a homogeneous solution formed. The extra oxalyl chloride and the toluene were distilled off. Fresh toluene (20 mL) was then transferred into the flask and distilled to remove any oxalyl chloride residue. The acid chloride was purified by using toluene and hexane (1/6, v/v) as cosolvents. Toluene (10 mL) and 60 mL of hexane were transferred into the flask followed by the addition of 1 g of anhydrous K<sub>2</sub>CO<sub>3</sub>. The solution was refluxed for 2 h under N<sub>2</sub>, and all insoluble compounds were removed by hot-filtration in a closed system. The filtered solution was then refluxed for 5 min and cooled slowly in the oil bath. Upon cooling, red crystals grew from solution. The mother liquor was filtered off, and the recrystallization of the acid chloride was repeated twice. The acid chloride crystal was then vacuum-dried for 8 h, dissolved in THF, and stored in a graduated reservoir before use. Mp: 94 °C. IR (KBr pellet): 1800 cm<sup>-1</sup> (acid chloride).

**5. Attachment of Mesogen to Polymer Backbone (Scheme 1).** A typical example is given below:

For the synthesis of LC-coil SICN5-66/60 (designated as SICN5-*x/y*, where S indicates polystyrene block, ICN5 indicates modified polyisoprene block (I) with cyanoazobenzene (CN) with a 5 methylene group spacer, *x* is the *M<sub>n</sub>* of the PS block, and *y* is the *M<sub>n</sub>* of the LC block in kilograms per mole), 0.50 g (0.52 mmol of OH) of the block copolymer was dissolved in 6 mL of anhydrous THF and 1 mL of pyridine. Immediately upon dropwise addition of the acid chloride (0.78 mmol in THF solution) at 0 °C, a white precipitate forms. Once the addition was complete, the solution was stirred for 24 h. The solution was then poured into 250 mL of ethanol/water (1:1 by volume), and the resultant yellow precipitate was filtered and subse-

quently washed with water and hot methanol. The polymer was collected and extracted with 95% ethanol using a Soxhlet extractor for 24 h. (The polymer can also be purified via a dissolve–reprecipitate cycle. Generally 5 cycles is enough to remove the small molecule mesogens. TLC indicates the absence of small molecule mesogenic groups.) Yield: 0.63 g (90%). *M<sub>n</sub>*: 223 000 g/mol (GPC). *M<sub>w</sub>*/*M<sub>n</sub>*: 1.15.

The attachment of side group mesogens to the hydroxylated poly(isoprene) homopolymer (0.15 g) is similar to the block copolymer attachment, except only pyridine is used as the solvent. Yield: 0.61 g (87.2%). *M<sub>n</sub>*: 68 000 (GPC). *M<sub>w</sub>*/*M<sub>n</sub>*: 1.15.

## Results and Discussion

**I. Anionic Polymerization.** Anionic polymerization of styrene and isoprene was chosen to prepare our starting materials to provide well-defined block copolymers with a narrow molecular weight distribution. Tetrahydrofuran (THF) was employed as the polymerization solvent in order to produce polyisoprene with a high pendent double-bond content. Styrene polymerizes very quickly in THF (within a few minutes) while isoprene polymerizes quite slowly (3 days are required for more than 90% conversion at –78 °C). To the best of our knowledge, no one has reported polyisoprene with 100% pendent double bonds while poly(1,2-butadiene) can be produced with 100% pendent double bonds by using the ligand dipiperidinoethane (DPE) in cyclohexane at 5 °C.<sup>27</sup> Poly(butadiene) with more than 99% 1,2-placement has been confirmed and widely used by other groups.<sup>28</sup> For poly(isoprene), such high pendent vinyl (and methylvinyl) content still remains a challenge. The lower toxicity and higher boiling point of isoprene provide other synthetic advantages, however.

The microstructure of the poly(isoprene) block was determined by <sup>1</sup>H NMR (400 MHz) and FT-IR as 39% 1,2-, 58% 3,4-, and 3% 1,4-double bond. This is consistent with Hashimoto's report,<sup>29</sup> although a slightly broader polydispersity (1.13–1.18) was reported in his paper. In the IR spectra, peaks observed at 910 and 996 cm<sup>-1</sup> are due to 1,2-double bonds (CH=CH<sub>2</sub>), the 886 cm<sup>-1</sup> peak is due to 3,4-double bonds, and the 864 cm<sup>-1</sup> peak is for the 1,4-double bonds. In the NMR spectra, the chemical shifts are assigned as follows: CH=C(CH<sub>3</sub>) (5.01 ppm), CH=CH<sub>2</sub> (5.71 ppm), CH=CH<sub>2</sub> (4.86 ppm), CH(CH<sub>3</sub>)=CH<sub>2</sub> (4.65 ppm).

In producing the poly(styrene-*b*-1,2- & -3,4-isoprene) diblock copolymer starting materials, the isoprene block was polymerized to nearly the same molecular weight of 10 000 g/mol (DP<sub>n</sub> = 147). The molecular weight of this block will increase by approximately 6 times after attachment of the mesogenic groups. By keeping the LC block the same DP<sub>n</sub>, we can eliminate the possible influence of molecular weight on LC behavior. The *M<sub>n</sub>* of the flexible coil block (polystyrene) was varied from 14 000 to 176 000 g/mol to cover a wide range of volume fractions in an attempt to produce different microdomain morphologies. The starting block copolymers are summarized in Table 1.

**II. Hydroboration.** The modification of a mono-dispersed polymer (both homopolymer and block copolymer) is always a challenging task due to possible side reactions if low polydispersity is to be retained. The hydroboration of polydiene homopolymers has been previously studied;<sup>24</sup> however, the results were far from satisfactory because of the presence of higher molecular weight fractions. In 1988, T. C. Chung<sup>22</sup> identified the branching side reaction of a modified polymer due to boric acid. He was able to remove trace amounts of boric

**Table 1. Summary of Properties of Starting Poly(1,2- & -3,4-isoprene) Homopolymer (I) and Poly(styrene-*b*-1,2- & -3,4-isoprene) Block Copolymers (SI)**

sample name	$M_n$ (GPC) <sup>a</sup>	$M_w/M_n$ <sup>a</sup>	theoretical $M_n$ (PS/PI) <sup>b</sup>
I-13	17 600	1.08	0/13 000 <sup>c</sup>
SI-14/13	36 000	1.07	14 400/12 700
SI-59/10	82 000	1.07	59 000/10 400
SI-66/10	81 000	1.06	66 000/10 200
SI-176/14	196 000	1.07	176 000/13 700
SI-176/9	190 000	1.07	176 000/9 300

<sup>a</sup> GPC calibration made using polystyrene standards. <sup>b</sup> The absolute molecular weight of the polystyrene precursor is measured by GPC using polystyrene standards. The molecular weight of the polyisoprene block is calculated from <sup>1</sup>H NMR in CDCl<sub>3</sub>. Therefore the numbers in this column are the absolute molecular weights. <sup>c</sup> Light scattering gives a  $M_n$  of 13 500 g/mol.

acid via distillation with methanol through the resultant azeotropic solution (with a boiling point of 58 °C). In the present system, this method only worked well for block copolymers with very short isoprene blocks. For the isoprene homopolymer, and block copolymers with short polystyrene blocks, it was not possible to retain narrow polydispersity using Chung's method. Therefore a series of model reactions were carried out in the presence of boric acid. Boric acid and methanol form a 1:3 complex, as established by NMR. Boric acid could also be distilled off with MeOH in the presence of DMF, but not in the presence of NaOH. Thus if the polymer solution remains basic, it is impossible to completely remove boric acid by distillation in the presence of methanol. This was especially true in the case of the polyisoprene homopolymer in which there is much more boric acid present than in the block copolymer. A purification method was developed by introducing a two-step purification which takes advantage of phase separation. After hydroboration and oxidation, the 'solution' was cooled to -78 °C, and the aqueous phase [NaB(OH)<sub>4</sub> and water] solidified as a fine powder while the organic layer remained in clear solution. When the 'solution' was warmed slowly to about 0 °C, the frozen aqueous layer (powder) formed a viscous syrup which could be easily separated from the organic layer by decanting. A second step was used to precipitate the hydroxylated block copolymer into a basic aqueous solution (0.2–0.3 M KOH or NaOH) as fine particles to avoid the hydrolysis of NaB(OH)<sub>4</sub>. After stirring at room temperature overnight, the polymer was filtered and redissolved in MeOH (for hydroxylated polyisoprene homopolymer) or THF/MeOH cosolvent (block copolymer) and reprecipitated 4 times into aqueous KOH solution (0.2–0.3 M). The polydispersity remained the same after hydroxylation, as shown in Figure 1.

It was necessary to esterify the hydroxyl groups of the homopolymer using acetyl chloride before GPC or NMR analysis, because the homopolymer was insoluble in THF. (It did dissolve in THF with a small amount of water.) The homopolymer was very soluble in MeOH, pyridine, DMSO, and DMF. The block copolymer with short hydroxylated isoprene blocks was very soluble in THF. As seen from the GPC traces (Figure 1), the apparent molecular weight of the hydroxylated polyisoprene block copolymer decreases relative to that of its parent block copolymer but retains the same polydispersity (1.07). This was due to intramolecular H-bonding, which leads to a decreased radius of gyration and therefore a smaller hydrodynamic volume.<sup>30</sup> <sup>1</sup>H NMR analysis showed the complete disappearance of pendent double bonds while the main chain double bonds remained (5.01 ppm), indicating quantitative

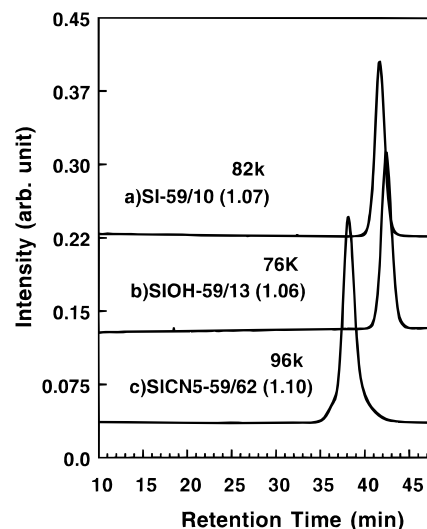


**Figure 1.** GPC traces of block copolymers: (a) starting poly(styrene-*b*-1,2- & -3,4-isoprene) block copolymer; (b) hydroxylated poly(styrene-*b*-1,2- & -3,4-isoprene) block copolymer after hydroboration/oxidation; (c) LC-coil diblock copolymer.

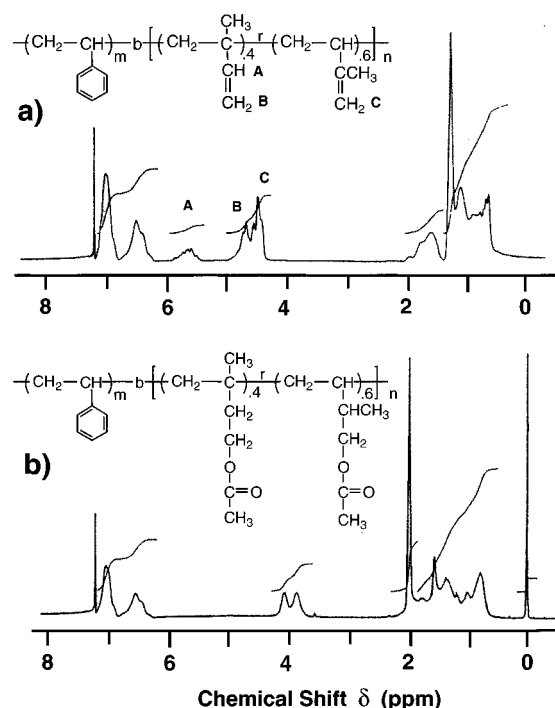


**Figure 2.** <sup>1</sup>H NMR spectra of starting poly(styrene-*b*-1,2- & -3,4-isoprene) block copolymer SI-14/13 before (a) and after (b) hydroboration. The hydroxylated block was capped with acetyl chloride to increase solubility.

hydroxylation of the pendent double bonds (Figure 2).

**III. Polymer-Analogous Chemistry: Attachment of Mesogenic Group.** Attachment reactions of the mesogenic group (see Scheme 1) utilizing the DCC coupling system were found to work very poorly, with only fractional conversion even with reaction times over one week. Acid chlorides were therefore employed to increase the extent of conversion and shorten the reaction time. To retain narrow polydispersity, the reaction conditions must be extremely clean, as any reactive species present can broaden the molecular weight distribution. We previously reported a method<sup>8</sup> in which thionyl chloride was used to synthesize acid chloride-terminated mesogens. In contrast to thionyl chloride we found that oxalyl chloride could be used to

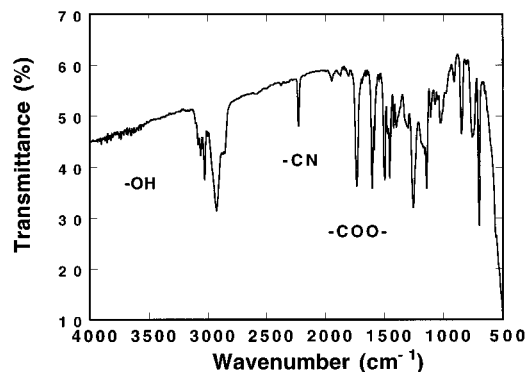


**Figure 3.** FT-IR spectrum of LC-coil diblock copolymer SICN5-66/60.

synthesize mesogenic acid chlorides which produced LC homo or block copolymers without any significant broadening of the molecular weight distribution.

Figure 3 shows a typical FT-IR spectrum of LC-coil diblock copolymer SICN5-66/60. The absorption peak of the hydroxyl group ( $3500\text{ cm}^{-1}$ ) completely disappeared in the modified polymer, indicating a high degree of mesogenic group attachment. A very strong ester group absorption peak appeared at  $1734\text{ cm}^{-1}$ . The peak at  $2222\text{ cm}^{-1}$  indicates the presence of the CN group of the mesogenic groups.  $^1\text{H}$  NMR data revealed more than 95% attachment, which is consistent with IR results.

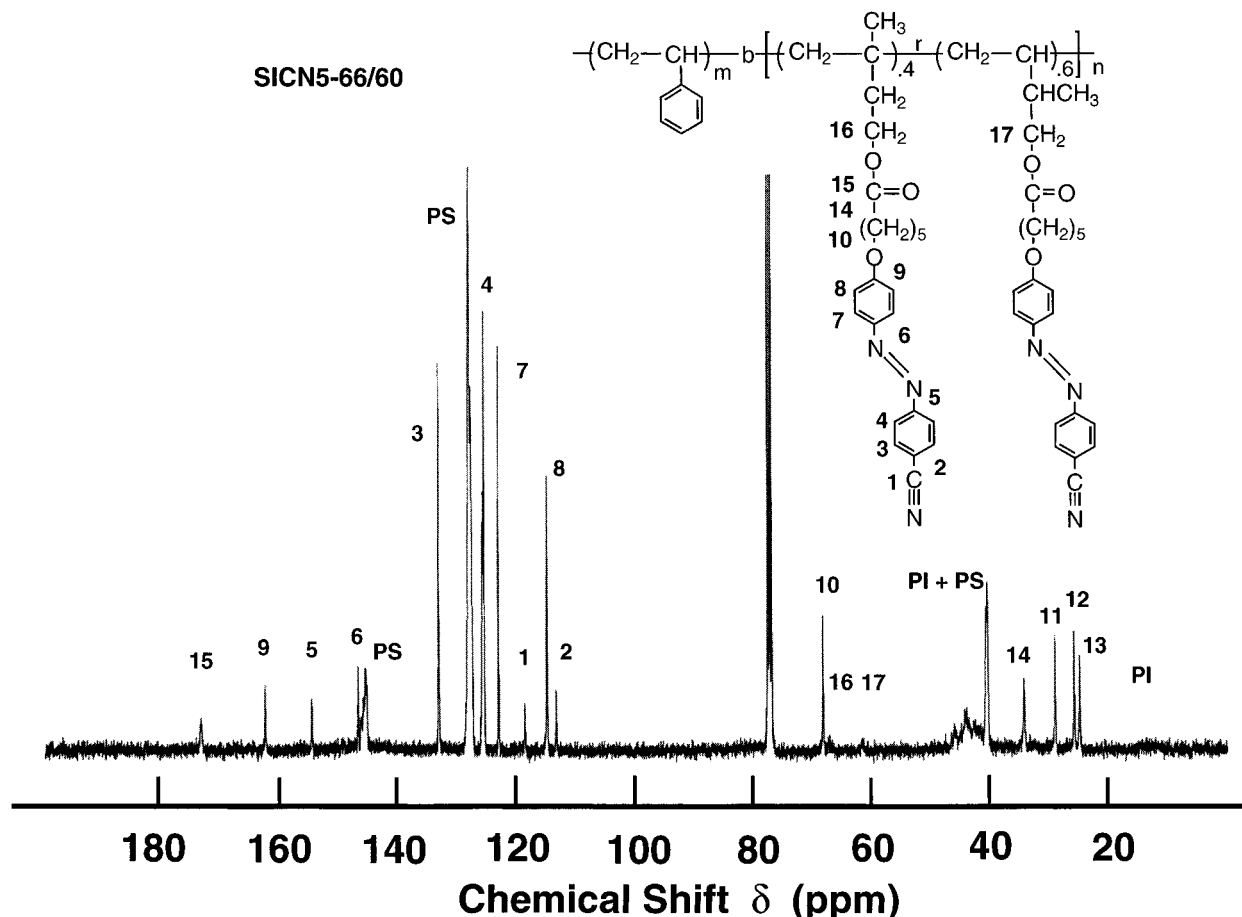
Figure 4 is the  $^{13}\text{C}$  NMR spectrum of LC-coil diblock copolymer SICN5-66/60. The assignments are shown in the figure. The chemical shift data are in good agreement with those calculated from the literature.<sup>31</sup>

The GPC and DSC results and sample information of the LC homopolymer and LC-coil diblock copolymers are summarized in Table 2.

**IV. Homopolymer Phase Behavior.** Figure 5 shows the DSC traces of homopolymer ICN5-78 with a  $T_g$  of  $45^\circ\text{C}$ , a smectic A mesophase, and a clearing transition temperature ( $T_i$ ) of  $178^\circ\text{C}$ . A higher order smectic phase exists between 45 and  $72^\circ\text{C}$ , as observed by DSC. Below  $T_g$ , the polymer is in the glassy LC state with a smectic mesophase. There is no crystallization upon annealing at temperatures slightly above  $T_g$ . The mesophase was determined by WAXD of a fiber drawn from the polymer melt (Figure 6). From WAXD, we find that the main chain axis aligned in the fiber axis direction while the mesogens packed together to form layers whose normal is orthogonal to the fiber axis. The smectic layer spacing is  $31\text{ \AA}$ , and the lateral distance between mesogens appears as a broad peak in the range  $4\text{--}5\text{ \AA}$  whose average is  $4.4\text{ \AA}$ .<sup>32</sup> From molecular modeling, the fully extended side group length is  $26.8\text{ \AA}$ . The observed  $31\text{ \AA}$  smectic  $d$ -spacing indicates partially interdigitated side group packing.

**V. Block Copolymer Properties.** The mesophases of the LC-coil diblock copolymers were also analyzed by DSC and WAXD. The microdomain structures were studied by SAXS and TEM.

All block copolymers including the block copolymer with  $f_{LC} = 0.22$  polystyrene were found to have a smectic A mesophase by WAXD analysis. On the basis of Fischer's phase diagram,<sup>7a</sup> one would expect a nematic phase with a spherical morphology for  $f_{LC} < 0.30$  block. However, as Figure 7 shows, a smectic mesophase with a  $31\text{ \AA}$   $d$ -spacing is observed. TEM revealed a LC-phase

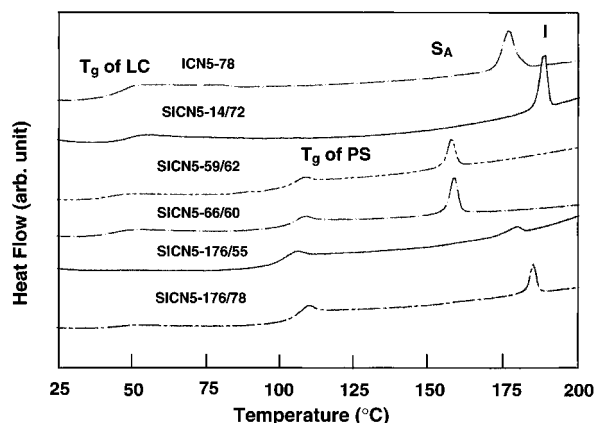
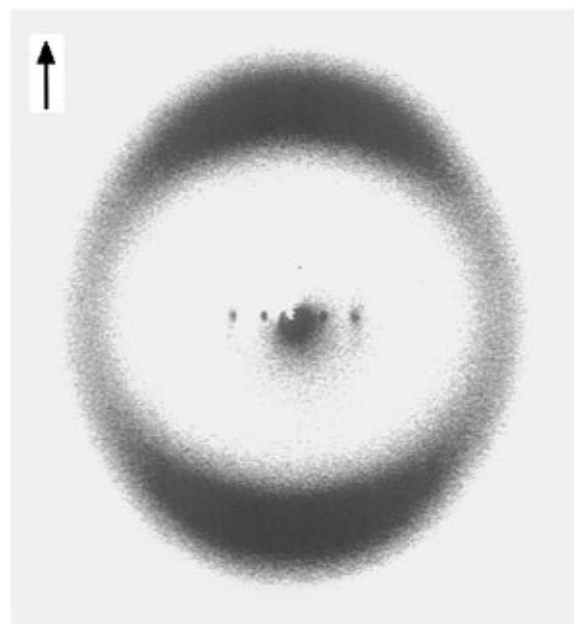


**Figure 4.**  $^{13}\text{C}$  NMR spectrum of LC-coil diblock copolymer SICN5-66/60.

**Table 2. Summary of LC-Coil Diblock Copolymers**

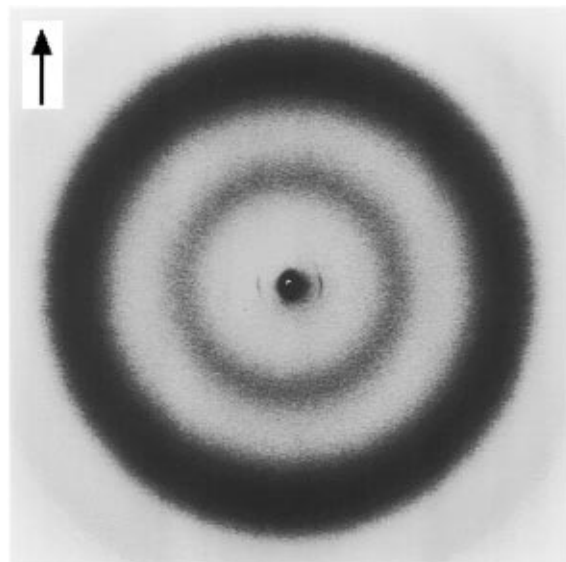
sample name	LC (wt %)	theoretical $M_n$ (PS/LC) <sup>a</sup>	GPC ( $M_w/M_n$ ) <sup>b</sup>	thermal transitions (°C) <sup>c</sup>	$\Delta H_{si}$ (J/g) <sup>d</sup>	obs morphology <sup>e</sup>
ICN5-78	100	0/78k	68k (1.15)	g45 S <sub>x</sub> 83 S <sub>A</sub> 176 I	4.40	Homo-Smectic A
SICN5-14/72	83.7	14k/72k (0.82) <sup>f</sup>	75k (1.24)	g45 S <sub>x</sub> 91 S <sub>A</sub> 188 I	4.33	CYL-Smectic A
SICN5-59/62	51.2	59k/62k (0.49)	96k (1.10)	g45 g101 S <sub>A</sub> 158 I	3.28	LAM-Smectic A
SICN5-66/60	47.6	66k/60k (0.45)	93k (1.12)	g45 g101 S <sub>A</sub> 157 I	3.17	LAM-Smectic A
SICN5-176/78	30.7	176k/78k (0.28)	223k (1.15)	g48 g103 S <sub>A</sub> 185 I	2.10	Bicontinuous-Smectic A
SICN5-176/55	23.8	176k/55k (0.22)	192k (1.13)	g45 g102 S <sub>A</sub> 179 I	1.93	CYL-Smectic A

<sup>a</sup> The absolute  $M_n$  of the polystyrene precursor is measured by GPC using polystyrene standards. The  $M_n$  of the LC block is calculated from <sup>1</sup>H NMR. <sup>b</sup> GPC calibration made using polystyrene standards. <sup>c</sup> From the DSC second heating. The mesophase is identified using WAXD. <sup>d</sup>  $\Delta H_{si}$  is for the LC block only. Data have been normalized according to the weight fraction of LC block. <sup>e</sup> LAM stands for lamella, and CYL stands for cylinder. <sup>f</sup> LC volume fraction ( $f_{LC}$ ).

**Figure 5.** DSC traces of LC homopolymer and LC-coil diblock copolymers.**Figure 6.** WAXD pattern of LC homopolymer ICN5-78. The fiber direction is shown in the figure.

cylindrical morphology (SICN5-176/55; Figure 12d) which had not been observed previously.<sup>7</sup> (More discussion of the morphology is given in section VI). This indicates that both the  $DP_n$  and domain size of the LC block play very important roles in determining the LC behavior of the LC-coil block copolymers and their microdomain structure.

The DSC traces (Figure 5) for all block copolymers (except sample SICN5-14/72 with a  $f_{LC} = 0.82$ ) exhibited two  $T_g$ 's: one at 45 °C for the LC block and one at 102 °C for the polystyrene block, indicating that the system is microphase-separated. The  $T_g$  of the polystyrene block increased slightly as its molecular weight in-

**Figure 7.** WAXD pattern of LC-coil diblock copolymer SICN5-176/55. The shear direction is shown in the figure.

creased. Block copolymers SICN5-59/62 and SICN5-66/60 (both are lamellar) showed  $T_i$  to be 18 °C lower than that of the LC homopolymer, while SICN5-14/72 (PS cylinder, Figure 12a) and SICN5-176/78 (bicontinuous Figure 12c) have *higher*  $T_i$  (12 and 9 °C higher, respectively) than the homopolymer. Sample SICN5-14/72 has a slightly broader polydispersity (1.24), which may explain its higher  $T_i$ . Comparing the two samples: SICN5-66/60 (lamellar,  $T_i = 157$  °C; Figure 12b) and SICN5-176/55 (LC block inside the cylindrical microdomain,  $T_i = 179$  °C; Figure 12d), the latter has a slightly lower  $M_n$  LC block but a 22 °C higher  $T_i$ . We believe this is due to confinement of the mesogenic group by the cylindrical microdomain structure which stabilizes the smectic mesophase within it. Detailed structural analysis of the LC cylinder phase is under investigation.

Figure 8 shows the normalized enthalpy change ( $\Delta H_{si}$ ) at the clearing transition ( $T_{SA} \rightarrow T_i$ ) vs PS content for the block copolymers. This behavior indicates that  $\Delta H_{si}$  has a strong dependence on block composition. In the lamellar regime, a 28% loss of enthalpy is observed from the homopolymer in contrast to Gronski's system, in which a 60% enthalpy loss was observed. In the LC cylinder regime (SICN5-176/55), a 56% enthalpy loss was detected. This indicates that the degree of enthalpy loss depends strongly on the system. The enthalpy loss in LC-coil diblock copolymers was originally believed to be due both to a disordered interface and to much smaller LC domains;<sup>6,7,13</sup> however, recent results<sup>33</sup> by Gronski et al. using <sup>2</sup>H NMR showed no evidence of an isotropic boundary layer at the LC-coil interface. Further study is required to clarify this phenomenon.

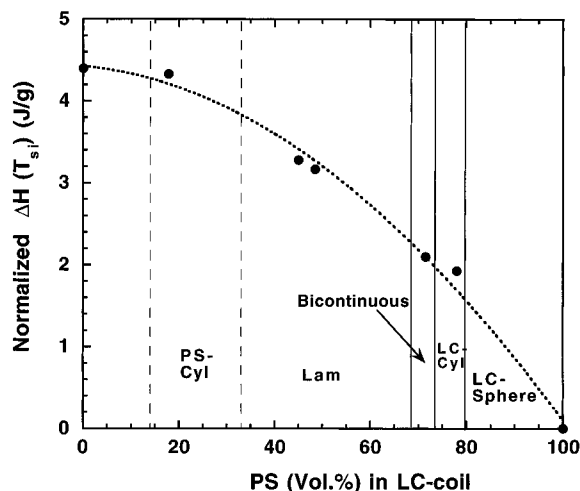


**Figure 8.** Normalized clearing transition enthalpy ( $S_A$  to isotropic) of LC-coil diblock copolymers vs block copolymer composition plot. A tentative phase diagram was also shown in the figure. (Sample SICN5-13/43 ( $f_{LC} = 0.75$ ) had a cylinder morphology<sup>38</sup>.) PS-Cyl stands for polystyrene cylinder; Lam for lamellae; LC-Cyl for LC cylinder.

**1. Interplay between Microdomain Structure and Liquid Crystallinity.** WAXD was employed to study the LC mesophase of our polymers. After shearing the LC-coil block copolymer sample SICN5-59/62 with a spatula, WAXD patterns clearly indicated that the mesogen axis was aligned perpendicular to the shear direction. The sharp inner arc corresponds to smectic layer distance (31 Å), but SAXS showed no lamellar orientation. After annealing the sheared sample at 140 °C (20 °C lower than  $T_i$ ), the mesogen lost all orientation, presumably due to the influence of the unoriented lamellae because the backbone of the block prefers to align normal to the interface. This observation also suggests that the microdomain structure is much harder to orient than the smectic layers, which is not surprising if we consider that the smectic layers have molecular level order while the microdomain structures are ordered at the supermolecular level.

When a sample with approximately equal volume fractions of LC and coil block (SICN5-66/60) was cast from 5 wt % toluene solution and slowly dried, oriented lamellae with an orientation parallel to the substrate were obtained, as indicated by SAXS (Figure 9, lamellar domain thickness  $L = 600$  Å). This is comparable to Hashimoto's results<sup>34</sup> on poly(styrene-*b*-isoprene) block copolymers. Interestingly, the mesogen was also oriented in this simple casting method, although not as well as in a sheared sample. This result indicates that the mesogen was oriented perpendicular to the polymer main chain, which was in turn perpendicular to the lamellar interface. This situation leads to smectic layer alignment perpendicular to the lamellar orientation in accordance with results from other LC-coil systems.<sup>6,7,13</sup> Watanabe et al.,<sup>13</sup> however, found no orientation in a solvent cast system, and SAXS studies showed only one scattering ring. Lamellae were oriented by pulling fibers from the polymer melt.<sup>13</sup> These observations are in contrast to our results and may be due to crystallization present in their system which dominates phase separation.

It was also observed that higher annealing temperatures gave better organization in these block copolymers. Smectic mesophases have relatively high viscosity; therefore, the mesogen could not be well-oriented with respect to the domain wall unless temperatures

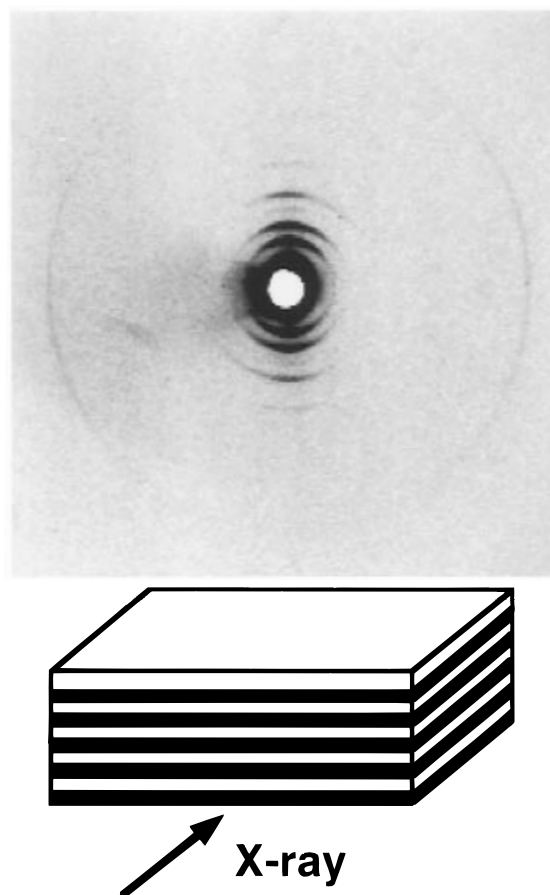


**Figure 9.** SAXS of LC-coil diblock copolymer SICN5-66/60. The sample was dried from toluene for 7 days and annealed at 145 °C (in the  $S_A$  mesophase) for 4 days.

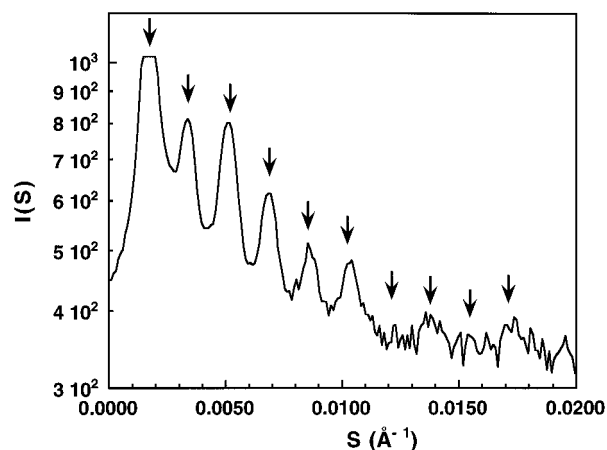


**Figure 10.** SAXS line scan (intensity vs. scattering vector) for SICN5-59/62. Peak orders of the lamellar microdomain are indicated with arrows.

approaching  $T_i$  were used. The mesogen becomes oriented parallel to the lamellar interface when using solvent-casting methods coupled with annealing. This fact indicates that the lamellar structure plays a very important role in determining mesogen orientation. The intermaterial dividing surface (IMDS) likely exerts a preferred homogeneous orientation upon the mesogens, which results in the alignment of the smectic layers normal to the lamellar layers.

**2. LC-Coil Interface Thickness.** A line scan of SAXS data for SICN5-59/62 is shown in Figure 10. Using Blundell's theory,<sup>35</sup> the simulation lead to a volume fraction of approximately  $f_{LC} = 0.46$  for the LC



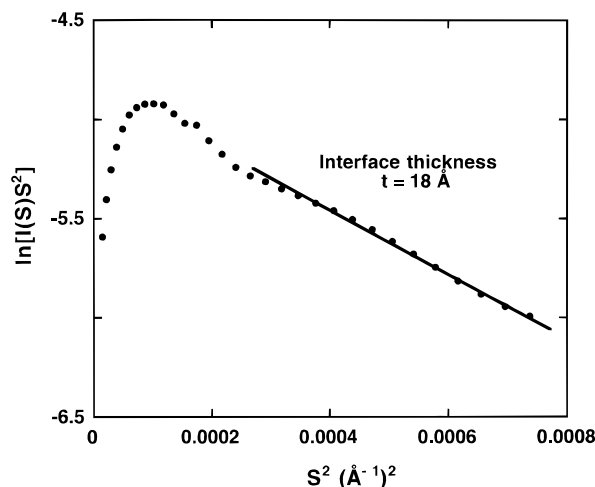


**Figure 11.** Plot of  $\ln[I(S)S^2]$  vs  $S^2$  for the interface thickness estimation of LC-coil diblock copolymer SICN5-59/62 (lamellar morphology).

block. For SICN5-66/60 ( $L = 580$  Å), the 5th and 7th orders are significantly weaker and simulation gave a volume fraction close to  $f_{LC} = 0.44$  for the LC block. Both of these values are in good agreement with the theoretical volume fractions calculated from density and molecular weight (0.49 and 0.45, respectively).

The interface thickness was calculated following the method of Hashimoto<sup>33,36</sup> by plotting  $\ln[I(S)S^2]$  vs  $S^2$  after subtracting background (Figure 11). Since  $I(S)S^2$  is proportional to  $\exp(-2\pi t^2 S^2)$  (where  $t$  is the interface thickness,  $S = (2 \sin \theta)/\lambda$ , and  $I(S)$  is intensity) and  $t = (|\text{slope}|/2\pi)^{0.5}$ , an interface thickness of 18 Å could be calculated for SICN5-59/62. These values are very similar to those found in poly(styrene-*b*-isoprene) systems<sup>33</sup> in which thicknesses of 17–20 Å are reported. Related semifluorinated block copolymers<sup>19b</sup> have a much sharper interface (11 Å). This is believed to be due to a much larger  $\chi$  parameter between polystyrene and the semifluorinated blocks.

#### VI. Microdomain Structure via TEM and SAXS.

Sample SICN5-14/72 ( $f_{LC} = 0.82$ ) exhibits a cylinder morphology with PS cylinders placed in a LC matrix. SAXS revealed a domain spacing  $D$  (distance between cylinders) of 375 Å and a cylinder radius ( $R$ ) of 85 Å, in good agreement with TEM observations (Figure 12a) which showed  $D = 390$  Å and cylinder radius  $R = 100$  Å.

TEM images of SICN5-66/60 (Figure 12b) revealed a microphase-separated lamellar morphology, as expected from the volume fraction of the LC block ( $f_{LC} = 0.45$ ). The lamellar domain spacing obtained from TEM was  $\sim 700$  Å, which is in fair agreement with SAXS results (600 Å).

A bicontinuous morphology was observed by TEM with sample SICN5-176/78 ( $f_{LC} = 0.28$ ) (Figure 12c).

TEM images of SICN5-176/55 (Figure 12d) showed a microphase-separated hexagonally packed cylinder morphology consistent with the volume fraction of the LC block of  $f_{LC} = 0.22$ . The cylinder domain spacing and radius obtained from TEM were 610 and 130 Å, respectively. From SAXS (Figure 13), the domain spacing ( $D$ ) was found to be 760 Å. On the basis of the LC volume fraction of 0.22, the cylinder radius was calculated to be 190 Å, in relatively good agreement with TEM data.

**1. Average Area per Junction for Coil Cylinder Morphology.** The average area per junction ( $\sigma_{jCYL}$ ) on the LC-coil interface for coil cylinder (PS domain)

morphology is given by

$$\sigma_{jCYL} = 2M_{PS}/(R_{CYL}\rho_{PS}N_{AV})$$

in which  $M_{PS}$  is the molecular weight of the PS block,  $R_{CYL}$  is the radius of the PS coil cylinder,  $\rho_{PS}$  is the density of the PS block, and  $N_{AV}$  is Avogadro's number. Using the domain size (375 Å) obtained from SAXS and volume fraction, cylinder radius was calculated to be 85 Å. Therefore, the calculated area per chain equals to 530 Å<sup>2</sup>, which implies that  $\sim 30$  block copolymer chains make up one smectic layer within the Wigner-Seitz cell of a single PS cylinder. Therefore the number of mesogens per chain is estimated to be 175 mesogens, which is in good agreement with the predicted  $DP_{LC} = 185$ . In Fischer's phase diagram,<sup>7a</sup> PS sphere morphology was observed for  $f_{PS}$  less than 30%, which is quite different from our observations, since our results clearly showed that a LC-coil diblock copolymer with  $f_{LC} = 0.82$  forms a cylinder morphology (by both TEM and SAXS). The cylinder morphology can offer a larger area per chain at the IMDS than a spherical morphology, a feature which is favorable for efficient packing of mesogenic groups at the IMDS. Therefore we expect that coil cylinder morphology can be formed with even higher LC volume fractions than 0.82 ( $f_{LC} > 0.82$ ).

**2. Average Area per Junction for Lamellar Morphology.** For the lamellar morphology, the average area per junction ( $\sigma_{jLAM}$ ) of the LC-coil interface is given by

$$\sigma_{jLAM} = 2M_{LC}/[N_{AV}\rho_{LC}(1 - f_{PS})L]$$

in which  $M_{LC}$  is the molecular weight of the LC block,  $\rho_{LC}$  is the density of the LC block,  $f_{PS}$  is the volume fraction of the PS block, and  $L$  is the lamellar spacing. From the SAXS results for SICN5-66/60, the volume fraction of the LC block ( $f_{LC}$ ) was found to be 0.44. Using this data and the 600 Å domain spacing obtained from SAXS, the area per chain at the styrene-LC intermaterial dividing surface was calculated to be approximately 640 Å<sup>2</sup>. In addition, from WAXD the length of the smectic layer of the side-group LC and the average intermesogen spacing were found to be 31 and 4.4 Å, respectively. These side-group dimensions suggest that the mesogens are arranged in a rectangular parallelepiped in which approximately 5 mesogens span the interface for a given block copolymer and about 30 mesogens are stacked away from the IMDS (Figure 14a). The width of the LC block and PS block domains is thus found to be approximately 270 Å and 330 Å, respectively, which is in good agreement with the SAXS results (260 and 340 Å).

**3. Average Area per Junction for LC Cylinder Morphology.** The average area per junction ( $\sigma_{jCYL}$ ) on the LC-coil interface for LC cylinder morphology is given by

$$\sigma_{jCYL} = 2M_{LC}/(R_{CYL}\rho_{LC}N_{AV})$$

in which  $R_{CYL}$  is the radius of the cylinder. For SICN5-176/55, an analysis similar to that shown above was carried out. Using the domain size, volume fraction, and cylinder radius obtained from SAXS, the area per chain at the LC cylinder IMDS was calculated to be 890 Å<sup>2</sup>. From this value, about 40 block copolymer chains were found to compose one smectic layer of a LC cylinder (Figure 14b). In addition, the pie-shaped wedge of volume per chain inside the cylinder was calculated

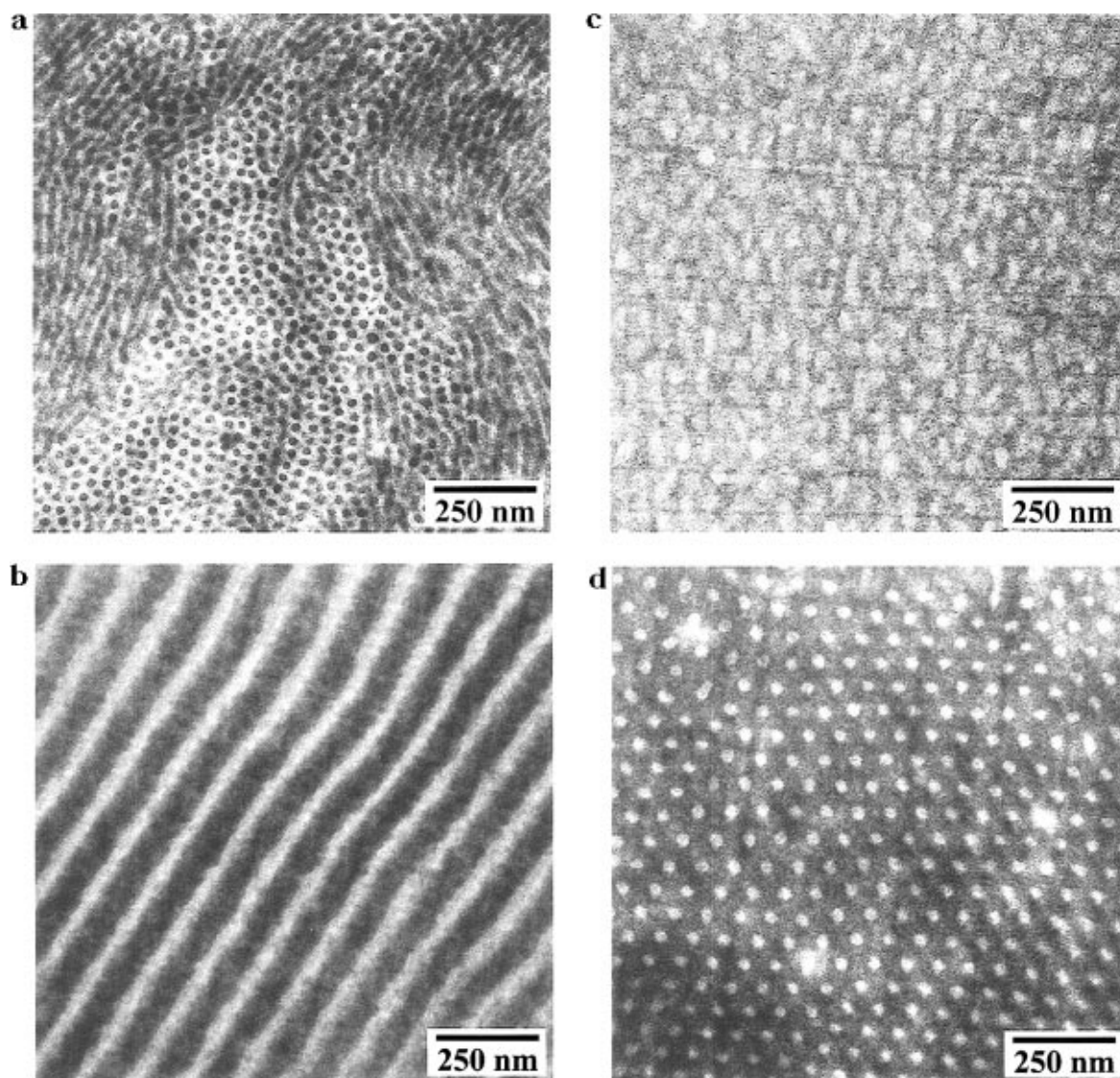


**Figure 12.** TEM images of LC-coil diblock copolymers: (a) SICN5-14/72, coil cylinder; (b) SICN5-66/60, lamellar; (c) SICN5-176/78, bicontinuous; (d) SICN5-176/55, LC cylinder. Samples were stained by RuO<sub>4</sub>, which preferentially stains the PS block.

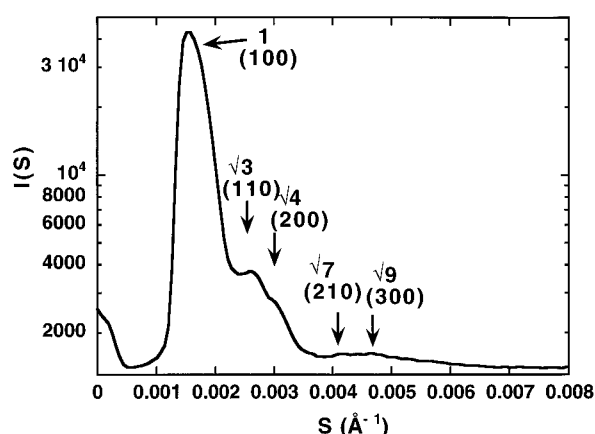


**Figure 13.** SAXS profile for SICN5-176/55. The peak index is shown in the figure.<sup>37</sup>

to contain  $\sim 130$  mesogens, which agrees well with the calculated number of mesogens per chain of 135 (assuming 100% attachment of side groups).

Figure 14c depicts a schematic representation of mesogen packing in a cylindrical subphase. The homogeneous packing model in which the mesogens all lie parallel to the IMDS is more probable (since we observe the homogeneous boundary alignment in the lamellar

LC-coil diblock) than the homeotropic packing in which the mesogens lie perpendicular to the IMDS based on space-filling considerations and the energy required to create a +1 disclination in the latter model. Such homogeneous orientation of the mesogen within the cylindrical microdomain may also stabilize the LC phase by raising the isotropization temperature due to confinement, since the order to disorder transition temperature of the LC-coil diblock greatly exceeds the LC clearing transition of the LC phase. Recent results by x-ray measurements (both WAXD and SAXS) of parallel plate processed LC cylinder samples indeed support our homogeneous model.<sup>38</sup>

We have also observed LC spheres by TEM of sample SICN5-107/29 ( $f_{LC} = 0.20$ ), which had a smectic mesophase, as indicated by WAXD. Detailed studies of the bicontinuous and the LC sphere morphologies are under investigation and will be reported elsewhere.<sup>38</sup> On the basis of the above results, a preliminary phase diagram is shown in Figure 8. More work is planned to explore both ends of the phase diagram.

## Conclusions

We have synthesized a series of LC-coil block copolymers containing azobenzene moieties via polymer analo-

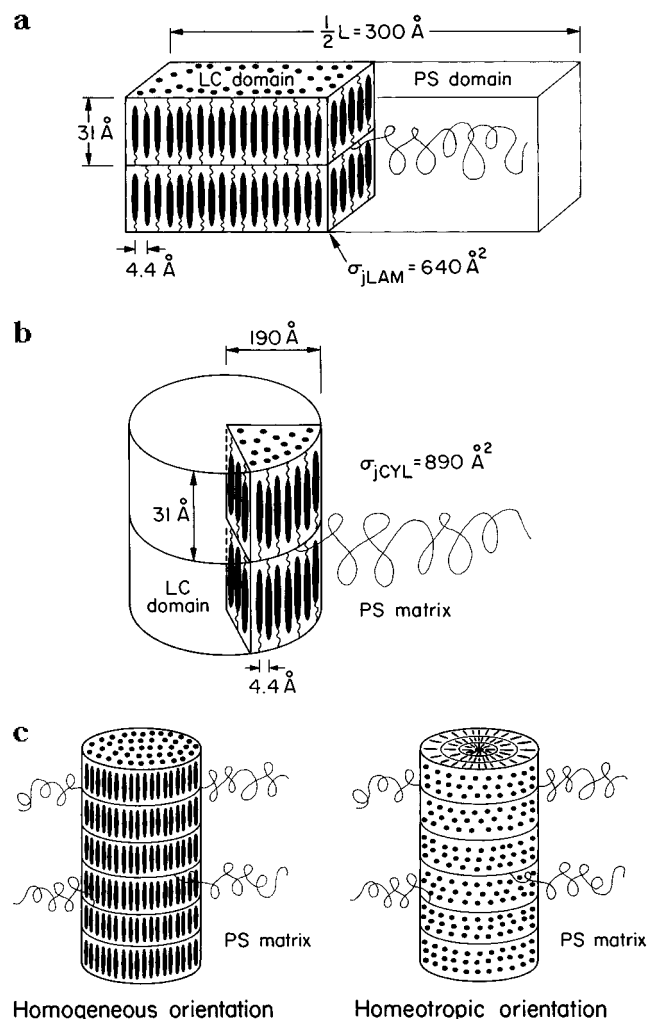


**Figure 14.** (a) Model for calculating area per chain for lamellar morphology. (b) Model for calculating area per chain for cylinder morphology. (c) Proposed structures of LC-cylinder in a PS matrix (with a  $S_A$  mesophase in the LC block): homogeneous (mesogen parallel to the IMDS) and homeotropic alignment (mesogen perpendicular to the IMDS).

gous chemistry starting from poly(styrene-*b*-1,2- & -3,4-isoprene). The LC-coil diblock copolymers were designed to have the same LC block molecular weight in order to eliminate any effect of variation of molecular weight on the LC behavior of the block copolymer. Morphological changes were produced by altering the  $M_n$  of the polystyrene block. Characterization of the mesophase showed that in addition to the LC homopolymer all the LC-coil block copolymers from  $f_{LC} = 0.82$  to  $f_{LC} = 0.20$  form smectic A mesophases. A LC cylinder morphology with smectic A cylinders embedded within a polystyrene matrix was observed for the first time in these LC-coil diblock copolymer systems ( $f_{LC} = 0.22$ ). The clearing transition of the cylinder phase is 22 °C higher than that for the LC phase in a lamellar structure even though the cylindrical domain sample has a slightly lower  $M_n$  for the LC block. We believe this is due to the cylindrical microdomain structure, which acts to stabilize the smectic mesophase within it.

By simple solvent-casting techniques, in polymers with roughly equal LC and polystyrene volume fractions, oriented lamellae could be formed with the lamellae direction parallel to the substrate surface while the mesogen was oriented homogeneously with respect to the IMDS. The presence of the mesogens causes increased chain stretching in the direction normal to

the IMDS. The interface thickness was estimated to be 18 Å, which is similar to that of conventional coil-coil diblock copolymers.

These studies provide further evidence that the interplay between a liquid crystalline phase and a microphase-separated structure presents a way of tailoring both the mesophase and the microstructure in such block materials. The area per chain, orientation of the mesogen with respect to the interface, and phase of the LC block can all be influenced by the volume fraction and design of the LC component. Other factors that one can use to tailor such structures include chain stiffness<sup>3b</sup> and surface free energy.<sup>19b,39</sup> Systematic investigations are underway to map out these influences.

**Acknowledgment.** Funding by NSF grants DMR94-01845 and DMR92-01845 is greatly acknowledged. G.M. would like to express his sincere thanks to M. J. O'Rourke for her collaboration and enlightening discussion, to Drs. D. R. Iyengar and S. S. Hwang for teaching him anionic polymerization, to Dr. H. Körner for his expertise in X-ray diffraction of LC polymers, to Drs. J. Adams, M. Brehmer, and H. K. Kim for their helpful discussion on polymer synthesis, to A. Shiota for his data analysis program for SAXS, and to the Ober CHESS team. We appreciate Dr. R. Albalak and Ms. Benita Dair for their help with LC-coil single crystal processing. S.R.C. would like to thank the Department of Education for a fellowship. We thank Dr. T. H. Mourey at Kodak for light-scattering measurements and CMSE-MIT, Cornell Materials Science Center (MSC), and CHESS for use of their facilities.

## References and Notes

- (1) *Developments in Block copolymers*; Goodman, I., Ed.; Applied Science: New York, 1982; Vol. 1.
- (2) (a) Bates, F. *Science* **1991**, *251*, 898. (b) Thomas, E. L.; Lescanec, R. L. *Philos. Trans. R. Soc. London, Ser. A* **1994**, *348*, 149. (c) Leibler, L. *Macromolecules* **1980**, *13*, 1602.
- (3) (a) Chen, J. T.; Thomas, E. L.; Ober, C. K.; Hwang, S. S. *Macromolecules* **1995**, *28*, 1688. (b) Chen, J. T.; Thomas, E. L.; Ober, C. K.; Mao, G. *Science* **1996**, *273*, 343. (c) Radziliński, L. H.; Wu, J. L.; Stupp, S. I. *Macromolecules* **1993**, *26*, 879.
- (4) (a) *Liquid-Crystalline Polymers*; Weiss, R. A., Ober, C. K., Eds.; ACS Symposium Series No. 435; American Chemical Society: Washington, DC, 1990. (b) Finkelmann, H.; Rehage, G. *Adv. Polym. Sci.* **1984**, *60/61*, 99. (c) Ober, C. K.; Jin, J.-I.; Zhou, Q.-F.; Lenz, R. W. *Adv. Polym. Sci.* **1984**, *59*, 102. (d) *Side Chain Liquid Crystal Polymers*; McArdle, C. B., Ed.; Chapman and Hall Press: New York, 1989. (e) *Liquid Crystal Polymers*; Plate, N. A., Ed.; Plenum: New York, 1992.
- (5) Chiellini, E.; Galli, G.; Angeloni, S.; Laus, M. *Trends Polym. Sci.* **1994**, *2*, 244.
- (6) (a) Adams, J.; Gronski, W. *Macromol. Chem., Rapid Commun.* **1989**, *10*, 553. (b) Adams, J.; Gronski, W. *ACS Symp. Ser. No. 435* **1990**, 174. (c) Adams, J.; Sanger, J.; Tefehne, C.; Gronski, W. *Macromol. Rapid Commun.* **1994**, *15*, 879.
- (7) (a) Fischer, H.; Poser, S.; Arnold, M.; Frank, W. *Macromolecules* **1994**, *27*, 7133. (b) Fischer, H.; Poser, S.; Arnold, M. *Liq. Cryst.* **1995**, *18*, 503. (c) Fischer, H.; Poser, S.; Arnold, M. *Macromolecules* **1995**, *28*, 6957. (d) Zschke, B.; Frank, W.; Fischer, H.; Schmutzler, K.; Arnold, M. *Polym. Bull.* **1991**, *27*, 1.
- (8) Mao, G.; Clingman, S. R.; Ober, C. K.; Long, T. E. *Polym. Prepr.* **1993**, *34* (2), 710.
- (9) Hefft, M.; Springer, J. *Macromol. Chem., Rapid Commun.* **1990**, *11*, 397.
- (10) Percec, V.; Lee, M. *J. Macromol. Sci., Pure Appl. Chem.* **1992**, *A29* (9), 723.
- (11) Komiya, Z.; Schrock, R. R. *Macromolecules* **1993**, *26*, 1387.
- (12) Bohnet, R.; Finkelmann, H. *Macromol. Chem. Phys.* **1994**, *195*, 689.
- (13) Yamada, M.; Iguchi, T.; Hirao, A.; Nakahama, S.; Watanabe, J. *Macromolecules* **1995**, *28*, 50.

- (14) Galli, G.; Chiellini, E.; Laus, M.; Bignozzi, M. C.; Angeloni, A. S. *Makromol. Chem. Phys.* **1994**, *195*, 2247.
- (15) (a) Frosini, A.; Levita, G.; Lupinacci, D.; Magagnini, P. L. *Mol. Cryst. Liq. Cryst.* **1981**, *66*, 21. (b) Percec, V.; Pugh, C. In *Side Chain Liquid Crystal Polymers*; McArdle, C. B., Ed.; Chapman and Hall: New York, 1989; Chapter 3.
- (16) Mao, G.; Ober, C. K. *Abstracts of the NERM (Northeast Regional Meeting of the American Chemical Society)*, Rochester, NY, 1995; American Chemical Society: Washington, DC, 1995; p 198.
- (17) Morton, M. *Anionic Polymerization*; Academic Press: New York, 1983.
- (18) Gabor, A. H.; Lehner, E.; Mao, G.; Schneggenburger, L. A.; Ober, C. K. *Chem. Mater.* **1994**, *6*, 927.
- (19) (a) Hwang, S. S.; Ober, C. K.; Perutz, S.; Iyengar, D. R.; Schneggenburger, L. A.; Kramer, E. J. *Polymer* **1995**, *36*, 1321. (b) Wang, J.; Mao, G.; Ober, C. K.; Kramer, E. J. *Macromolecules* **1997**, *30*, 1906.
- (20) Still, W. C.; Kahn, M.; Mitra, M. *J. Org. Chem.* **1978**, *43*, 2923.
- (21) (a) Morton, M.; Fetters, L. J. *Rubber Chem. Technol.* **1975**, *48*, 359. (b) Fetters, L. J. *J. Res. Natl. Bur. Stand., Ser. A* **1966**, *70A* (5), 421. (c) Bywaters, S. In *Comprehensive Polymer Science*; Eastmond, G., Ledwith, A., Russo, S., Sigwalt, P., Eds.; Pergamon Press, Inc.: New York, 1989; Vol. 3, Chapter 28, pp 433–447.
- (22) Chung, T. C.; Raate, M.; Berluche, R. E.; Schulz, D. N. *Macromolecules* **1988**, *21*, 1903.
- (23) Kendall, E. W.; McCarthy, T. J. *Polym. Prepr.* **1992**, *33* (2), 158.
- (24) Pinazzi, C.; Brosse, J. C.; Pleurdeua, A.; Reyx, D. *Appl. Polym. Symp.* **1975**, *26*, 50.
- (25) (a) Ringsdorf, H.; Schmidt, H. W. *Macromol. Chem.* **1984**, *185*, 1327. (b) Hsiue, G.-H.; Wen, J.-S.; Hsu, C.-S. *Polym. Bull.* **1993**, *30*, 141. (c) Aoki, K.; Tamami, T.; Seki, T.; Kawanishi, Y.; Ichimura, K. *Langmuir* **1992**, *8*, 1014 and 1007.
- (26) (a) Coleman, G. H.; Nichols, G.; McCloskey, C. M.; Ansporn, H. D.; Bachmann, W. E.; Deno, N. C. *Org. Synth.* **1955**, Collect. 3, p 712. (b) Adams, R.; Ulich, L. H. *J. Am. Chem. Soc.* **1920**, *42*, 599.
- (27) Hals, A. F.; Lohr, D. F.; Hall, J. F. *J. Polym. Sci., Polym. Chem. Ed.* **1981**, *19*, 1357.
- (28) (a) Xu, Z.; Hadjichristidis, N.; Carella, J. M.; Fetters, L. J. *Macromolecules* **1983**, *16*, 925. (b) Bates, F. S.; Fetters, L. J.; Wignall, G. D. *Macromolecules* **1988**, *21*, 1086.
- (29) Hashimoto, T.; Nakamura, N.; Shibayama, M.; Izumi, A.; Kawai, H. *J. Macromol. Soc., Phys.* **1980**, *B17* (3), 389.
- (30) Tuzar, Z.; Kratochvil, R. In *Surface and Colloid Science*; Matijevic, E., Ed.; Plenum Press: New York, 1993; Vol. 15, Chapter 1, p 1.
- (31) Clerc, J. T.; Pretsch, E.; Seibl, J. *Structural Analysis of Organic Compounds by Combined Application of Spectroscopic Methods*; Elsevier Scientific Publishing Company: New York, 1981.
- (32) Freidzon, Ya. S.; Talroze, R. V.; Boiko, N. I.; Kostromin, S. G.; Shibaev, V. P.; Plate, N. A. *Liq. Cryst.* **1988**, *3* (1), 127.
- (33) Martin, A.; Tefehne, C.; Gronski, W. *Macromol. Rapid Commun.* **1996**, *17*, 305.
- (34) Hashimoto, T.; Shibayama, M.; Kawai, H. *Macromolecules* **1980**, *13*, 1237.
- (35) Blundell, D. J. *Acta. Crystallogr., Ser. A* **1970**, *26*, 466 and 472.
- (36) Hashimoto, T.; Shibayama, M.; Fujimura, M.; Kawai, H. In *Block Copolymers Science and Technology*; Meier, D. J., Ed.; MMI Press and Harwood Academic Publishers: New York, 1983; p 63.
- (37) The SAXS peaks are indexed as shown in Figure 14, which correspond to  $d$ -spacings of 655 ( $d_1$ , 100), 382 (110), 330 (200), 244 (210), and 214 Å (300), respectively. Therefore the domain spacing  $D$  (distance between cylinders) is equal to  $d_1$  times  $2/\sqrt{3} = 757$  Å. From a volume fraction of 0.22, the expected cylinder radius ( $R_{CYL}$ ) is  $(0.276f_{LC})^{0.5}D = 186$  Å.
- (38) Mao, G.; Ober, C. K.; Chen, J. T.; Thomas, E. L. Unpublished results.
- (39) Ober, C. K.; Wang, J.; Mao, G.; Kramer, E. J.; Chen, J. T.; Thomas, E. L. *Macromol. Symp.*, in press.

MA9617835